Current issues for the internal stability design of geosynthetic reinforced soil

Bathurst, R.J.
Professor, GeoEngineering Centre at Queen's-RMC, Department of Civil Engineering, Royal Military College of Canada, Kingston, Ontario, K7K 7B4, Canada

Allen, T.M.
State Geotechnical Engineer, Washington State Department of Transportation, State Materials Laboratory, Olympia, Washington, 98504-7365, USA

Huang, B.Q.
GeoEngineering Centre at Queen's-RMC, Department of Civil Engineering, Queen's University ,Kingston, Ontario, K7L 3N6, Canada

Keywords: reinforced soil walls, limit equilibrium, Simplified Method, K-stiffness Method, limit states design

ABSTRACT: Current design methods for the internal stability analysis of geosynthetic reinforced soil walls are based on limit equilibrium analysis and the assumption of a simultaneous failure state for the soil and reinforcement. The paper reviews deficiencies in the use of strength-based analyses for reinforcement rupture and pullout design of walls under operational conditions. Measured and predicted reinforcement loads using the current North American Simplified (tie-back wedge) Method are compared and predicted values shown to be very poor on average. Sources of poor prediction accuracy are identified using results of instrumented full-scale walls and numerical modeling. The essential features of a new empirical-based working stress design method (K-stiffness Method) are presented. This new method explicitly includes the influence of reinforcement stiffness and the structural facing amongst other contributions. Statistical analysis of the bias of measured to predicted load is used to demonstrate the improved accuracy of this new load design approach. Finally, the paper discusses the implications of load model accuracy on reliability-based limit states design calibration.

1 INTRODUCTION

Geosynthetic reinforced soil walls have been in use since the 1970s and they are now a well-established technology for retaining wall applications. The popularity of these systems has been driven by economics. For example, geosynthetic reinforced soil walls have been demonstrated to be about 50% of the cost of conventional (gravity) retaining wall systems (Koerner et al. 1998).
Nevertheless, there are a number of challenges and issues related to our understanding of the behavior of these systems and the development of the next generation of calibrated internal stability design methods using reliability-based theory. This paper discusses some of these issues including the role of the empirical-based K-stiffness Method for the calculation of loads in future generations of reliability-based limit states design methods for geosynthetic reinforced soil retaining walls.

2 LIMIT EQUILIBRIUM DESIGN METHODS

2.1 *General*

Current design methods for reinforced soil walls that appear in design guidance documents are based on extensions of classical limit equilibrium theory (e.g. AASHTO 2002, 2007; FHWA 2001; BS8006 1995; CFEM 2006; Geoguide 6 2002, NCMA 2009; PWRC 2000). Simply stated, these methods are based on models that assume the backfill soil is at a failure state consistent with the notion of plasticity and at the same time there is a corresponding and simultaneous failure mechanism developed in one or more reinforcing elements (e.g. reinforcement rupture or pullout). The application of limit equilibrium theory to design leads to the assumption of a contiguous internal failure mechanism through the reinforced soil zone defined by a wedge, bi-linear wedge or circular slip surface.

In North America, the Simplified Method for geosynthetic walls was developed from the tie-back wedge method used to design the earliest geosynthetic walls in the 1970s (Whitcomb and Bell 1979). The tie-back wedge method was based on the concept used by Vidal for internal stability design of steel reinforced walls. The tie back wedge method initially used the coefficient of earth pressure-at-rest (K_o) to compute the earth pressures/forces carried by the reinforcement layers and then a few years later the coefficient of active earth pressure (K_a) was adopted for the entire full height of the geosynthetic wall.

The Coherent Gravity Method assumes a bilinear failure block for internal stability design and can be understood to be a variant of the single wedge approach. Nevertheless, semi-empirical adjustments to the computed earth pressure coefficient were required to give a reasonable match between measured steel reinforcement loads under operational conditions and predicted values. Here, the term "operational conditions" refer to working stress conditions. For reasons discussed later these conditions correspond essentially to the end of construction provided that site conditions and boundary load conditions do not vary over the life of the structure (the typical assumption for earth structures in static load environments). Without the empirical adjustments noted above, the observed generally good agreement between measured reinforcement loads in steel reinforced soil walls under operational conditions and design predictions is not possible. Recent statistical analysis of steel reinforcement loads using the AASHTO Simplified Method and the Coherent Gravity Method has confirmed the generally good agreement between design theory and measured loads (Bathurst et al. 2008b, 2009). Nevertheless, some improvement between observed and measured reinforcement loads in steel reinforced soil walls is possible by using an empirical-based working stress method that accounts for the reinforcement stiffness (Allen et al. 2004).

To the best of the writers' knowledge the accuracy of the AASHTO Simplified Method (i.e. tie-back wedge method) for geosynthetic reinforced soils was never validated against best estimates of reinforcement loads taken from instrumented walls before it was adopted in current North American design codes. One reason was that there were very few instrumented walls available in the late 70s and early 80s. Furthermore, strategies to estimate reinforcement loads from strain measurements were not available. Nevertheless, the opinion of experienced design engineers at that time (and continues today) was that the AASHTO Simplified Method gave computed reinforcement load values that were conservative (i.e. safe) for design (e.g. Allen and Holtz 1991; Rowe and Ho 1993; Allen et al. 2002).

While the general approach is safe it is not accurate (on average) as demonstrated later in the paper. There are a number of disadvantages of limit equilibrium-based methods for internal stability design of geosynthetic reinforced soil walls which contribute to their poor prediction accuracy. For example, Leshchinsky and Han (2003) identified the following shortcomings of limit equilibrium-based methods:

1) Equilibrium is satisfied only for sliding mass modes of failure;
2) Deformation is not considered;
3) In simplified methods, failure is allowed only on predefined surfaces; and
4) Kinematics are not considered so that some failure mechanisms may not be possible.

Hence, if reinforced soil walls are assumed *a priori* to be at incipient collapse for design purposes, the general approach has major deficiencies. In fact, walls are designed for working stress conditions. Given the points made above it cannot be accepted that limit equilibrium-based methods of analysis for internal design of reinforced soil walls are rational. It is more appropriate to understand that this general approach results in simple models that do not satisfy a consistent mechanics framework but nevertheless result in conservative (safe) designs. Furthermore, the complex interactions that develop between a structural facing (a common feature of permanent walls) and the soil and reinforcement cannot be captured using simple wedge or slip surface models based only on force-equilibrium. The persistence of limit equilibrium-based models for the internal stability design of geosynthetic reinforced design in current design codes is largely the result of lack of an alternative analytical approach. Nevertheless, the earliest attempts in North America to improve the prediction accuracy of geosynthetic reinforcement loads under operational conditions recognized that reinforcement loads were a function of displacement and hence the tensile stiffness of the reinforcement is a fundamental property for design (Christopher 1990, 1993). An obvious shortcoming of limit-equilibrium methods that consider only the strength of the reinforcing elements is that predicted loads under operational conditions will be the same for steel and relatively extensible polymeric materials provided they have the same strength and number of layers in the wall.

2.2 *Reinforcement loads under operational conditions*

The writers and co-workers have collected data from 31 instrumented geosynthetic reinforced soil walls (Allen and Bathurst 2002; Allen et al. 2003; Bathurst et al. 2005, 2008b). Of these case studies a total of 13 structures were constructed with cohesionless backfill soils.

Walters et al. (2002) developed a method to estimate geosynthetic reinforcement loads in instrumented walls using a suitably selected secant stiffness value (J) from in-isolation constant load (creep), constant rate-of-strain (CRS) or constant strain (relaxation) tests. Secant stiffness values corresponding to 2% strain are plotted against time in Figure 1. The secant stiffness value used to estimate reinforcement loads in instrumented walls was selected based on measured strain (ε) and duration of tensile loading (t) at the point of maximum internal strain in the wall. Hence, the maximum reinforcement tensile load T_{max} can be computed as:

$$T_{max} = J(\varepsilon, t) \times \varepsilon \qquad (1)$$

The accuracy of this approach was confirmed by comparing estimated loads using the secant stiffness approach with directly measured loads in the reinforcement where these two sets of measurements were available (Walters et al 2002; Bathurst et al. 2005).

Measured loads based on interpretation of reinforcement strains are plotted against calculated loads in Figure 2. The predicted (calculated) loads were computed using the AASHTO Simplified Method:

$$T_{max} = K\sigma_v S_v \qquad (2)$$

Here, K is the horizontal component of the active earth pressure coefficient, σ_v is the vertical stress at the reinforcement elevation and S_v is the reinforcement vertical spacing. The data show that *on average* the measured loads are about one third of the computed values. The accuracy of the predicted loads is also poor based on the ratio of measured to predicted loads – called load bias. The

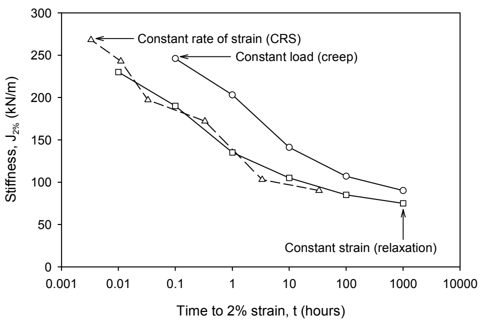

Figure 1. Secant stiffness values from in-isolation testing of polypropylene (PP) geogrid specimens (Bathurst et al. 2005).

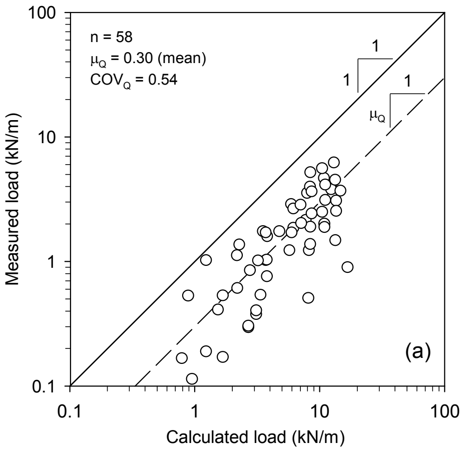

Figure 2. Measured reinforcement load versus calculated load using AASHTO Simplified Method.

spread (scatter) in the ratio of measured to predicted load (using the coefficient of variation of this ratio) is greater than 50%. In fact, the calculated loads were computed using the peak plane strain friction angle of the backfill soil. In practice, engineers use the peak triaxial or direct shear friction angle for design which is less than the plane strain values used in this comparison. In some cases designers use the residual friction angle of the soil which is even lower. Hence, in practice the predicted maximum reinforcement loads will be less and the accuracy of the AASHTO Simplified Method to predict reinforcement loads under operational conditions even poorer and more conservative. Furthermore, the distribution of loads does not increase linearly with depth as predicted using the Simplified Method. Figure 3 shows normalized load data for measured and predicted values at end of construction using the current Simplified Method and cohesionless soils. The maximum load T_{max} in a reinforcement layer is normalized with T_{mxmx} which is the maximum reinforcement load in the wall, and the reinforcement depth (z + S) is

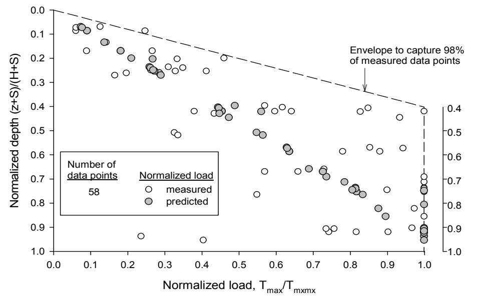

Figure 3. Normalized distribution of measured and predicted reinforcement loads for walls with cohesionless backfill soil.

normalized with equivalent height of wall (H + S) where H is the height of the reinforced soil zone (wall) and S is the equivalent height of uniform surcharge pressure (if applicable). The deviation of the predicted load values from a straight line is because some walls did not have uniform reinforcement spacing at all layers. It is clear that the general trend towards increasing T_{max} with depth using the AASHTO Simplified Method falls well within the envelope that captures 98% of the measured data. The large spread in the load bias data (i.e. large COV_Q values) is due to the wide range of over-estimated and under-estimated measured loads with respect to predicted values. The underlying deterministic model does poorly to capture both the trend in the distribution of load data with depth and the magnitude of load in each reinforcement layer for walls under operational conditions.

3 SOURCES OF CONSERVATISM IN CURRENT PRACTICE

In the previous section the over-prediction of reinforcement loads using the Simplified Method has been identified. Here we identify some sources of this conservatism and the reasons for the bi-linear distribution of reinforcement loads shown in Figure 3.

3.1 *Influence of facing stiffness and toe support*

The influence of facing type on the performance of the RMC walls was reported by Bathurst et al. (2006). Wall 1 (Figure 4a) was constructed with a relatively stiff modular block facing and Wall 4 (Figure 4b) with a very flexible wrapped-face construction. In most design guidance documents the structural capacity of a hard facing with good toe support is ignored in the computation of reinforcement load. An example is the current AASHTO (2002) Simplified Method (tie-back wedge method) and BS8006 (1995). These methods and variants use a contributory earth pressure approach to assign active earth loads to each reinforcement layer (Equation 2).

For the two walls shown in Figure 4, predicted T_{max} load values were calculated using three different peak friction values for the backfill soil ($\phi = \phi_{ps}$ (plane strain) > ϕ_{ds} (direct shear) > ϕ_{cv} (constant volume)) determined from laboratory direct shear and plane strain tests and wall-soil interface friction angle $\delta = \phi$. The results of these calculations appear as the linear lines in Figures 5a and 5b. To make fair comparisons between walls with and without a hard face the conservative assumption (i.e. safer for design) was made to assume a soil-

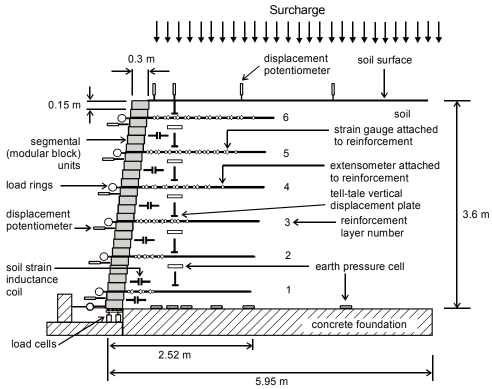

a) hard-face wall showing instrumentation (Wall 1)

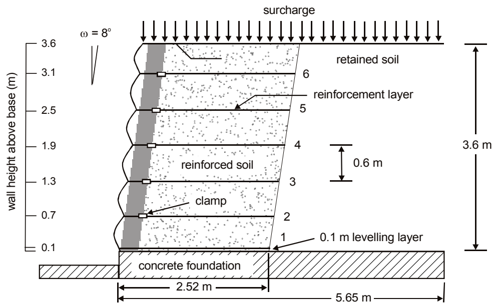

b) wrapped-face wall (Wall 4)

Figure 4. Example RMC full-scale reinforced soil walls.

to-soil interface inclined at $\omega = 8°$ for the wrapped-face wall and located 0.3 m from the face of the wall (i.e. at the location of the clamps shown in Figure 4b). Predicted load values at each surcharge load level can be seen to decrease with increasing peak friction angle as expected using Coulomb earth pressure theory. The peak friction angle (ϕ_{ds}) from direct shear tests (or conventional triaxial compression tests) is specified in current North American practice (AASHTO 2002, NCMA 2009). Allen et al. (2002) have proposed that the peak plane strain angle (ϕ_{ps}) be used in current reinforced soil wall design practice (tie-back wedge method) since wall geometry typically conforms to a plane strain condition. Furthermore, lower reinforcement loads are predicted which reduces the discrepancy with observed loads in field walls that have been inferred from measured strains. Indeed, the data for the hard-face (segmental) wall in Figure 4a shows that the least discrepancy between predicted and measured reinforcement loads at all surcharge levels corresponds to calculations using the peak plane strain friction angle ($\phi = \phi_{ps}$). The magnitude of the discrepancy between predicted and measured results increases as the value of ϕ decreases.

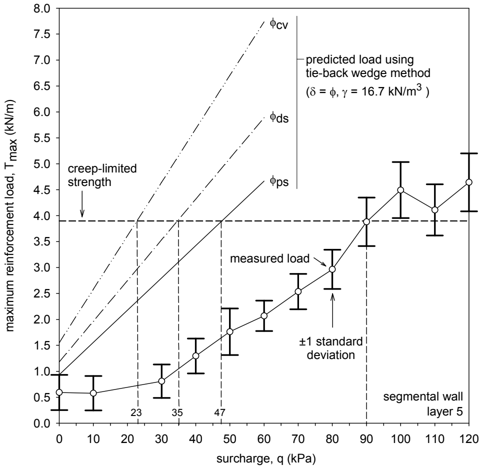

a) hard-face wall (Wall 1)

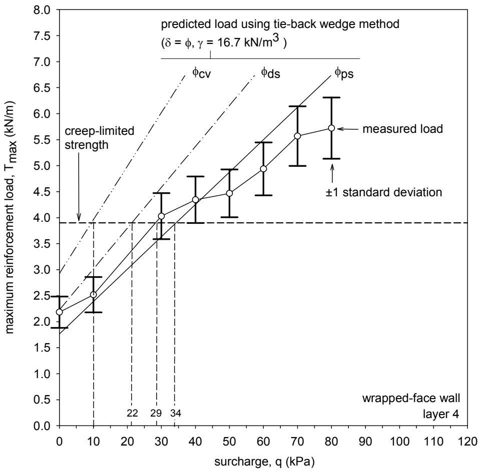

b) wrapped-face wall (Wall 4)

Figure 5. Predicted and measured maximum reinforcement tensile loads at end of construction and during surcharging for hard-face segmental wall and flexible wrapped-face wall.

Superimposed on the figures is the creep-limited strength for the reinforcement (3.9 kN/m). The creep-limited strength value is a limit state for design since it represents a reinforcement tensile load that if sustained over a long period of time can be expected to lead to strain to rupture of the layer. The measured data show that the creep-limited strength of the critical reinforcement layer in Wall 1 was reached at a surcharge load of 90 kPa while predicted surcharge levels to reach this limit state are 47, 35 and 23 kPa for calculations carried out with ϕ equal to ϕ_{ps} , ϕ_{ds} and ϕ_{cv} , respectively. Hence, the surcharge load level required to reach this limit state is under-predicted by a factor of 1.9, 2.6 and 3.9 for the hard-face wall structure using ϕ equal to ϕ_{ps} , ϕ_{ds} and ϕ_{cv} , respectively.

A similar set of data are shown in Figure 5b for the flexible wrapped-face wall structure. The surcharge load level to reach the creep-limited strength limit state is 29 kPa which is 3.1 times less than the value of 90 kPa for the nominally identical stiff-face wall. This difference is ascribed to the relatively low facing column stiffness for the flexible wrapped-face wall structure. It can be noted that the tie-back wedge method using the peak plane strain friction angle ($\phi = \phi_{ps}$) gives reasonably accurate estimates of measured reinforcement loads (i.e. generally within ±1 standard deviation of the mean measured load value) for surcharge levels up to 50 kPa. At end of construction the peak direct shear value calculation with $\phi = \phi_{ds}$ gives a value of maximum reinforcement load that matches the measured value but over-estimates the measured values during subsequent surcharging. Within experimental error it can be argued that the surcharge load to reach the creep-limited strength value of the reinforcement falls within limits predicted using peak direct shear and peak plane strain friction angles for the soil (ϕ_{ds} = 41° and ϕ_{ps} = 44°, respectively). Calculations using $\phi = \phi_{cv}$ under-estimated the surcharge load level to achieve the creep-limited strength of the critical layer by a factor of 2.9. While not shown here, wall deformations were also higher for the flexible face wall than for the nominally identical wall with a hard facing, demonstrating that the facing column acted as a structural member to carry a portion of the earth load acting against the face.

It should be noted however, that the RMC wrapped-face wall is an unusually flexible structure. It was purposely designed to encourage a soil failure mechanism at end of construction. This objective was met. However, wrapped-face wall structures in practice are constructed with facing wraps that extend into the reinforced soil zone and this can be expected to give a stiffer facing performance. The soil reinforcement material used in this test wall was also very extensible. Hence, the surcharge pressure to achieve the same performance limit state can be expected to be greater for a similar height wrapped-face structure in the field constructed with stiffer geogrid reinforcement. Consequently, it may be expected that the agreement between predicted peak maximum reinforcement load and the measured load would be closest using a peak plane strain friction angle for a wall built with facing wraps that extend back into the soil.

A major important conclusion from the analysis of these two walls was that by using the peak plane strain friction angle of the sand backfill in reinforcement load calculations, the maximum load in the reinforcement layers for the very flexible wrapped-face wall was reasonably well predicted using the current AASHTO Simplified Method (AASHTO 2002). Hence, for this idealized case, fundamental limit equilibrium concepts can be argued to apply. However, reinforcement loads were over-predicted using the same method applied to the wall with the hard facing. Clearly, the hard facing was a structural element that added to the earth load capacity of the wall. However, this contribution requires that there be sufficient restraint at the toe of the wall facing column. In the RMC walls with a hard face, the toe of the wall was seated on a set of frictionless linear bearings to decouple the measured horizontal and vertical toe loads. The toe was restrained in the horizontal direction using load rings that nevertheless had a measureable compliance (i.e. were not perfectly rigid) (Figure 4a).

To examine the potential load capacity at the toe of the wall a series of full-scale laboratory direct shear tests were carried out using smooth bottom concrete blocks placed on a flat concrete surface (footing) and two different crushed stone aggregate leveling pads (Huang et al. 2010). The shear tests showed that a horizontal movement of 2 mm matching the value observed at the toe of the hard faced wall at the end of construction gave the same horizontal load as that measured in the full-scale wall test. Hence, the magnitude of horizontal load developed at the supported toe in the RMC wall test is judged to be reasonable for these systems in the field provided that the foundation soil below the leveling pad or concrete footing is stiff and competent. In a program of complementary numerical modeling, the horizontal toe restraint was simulated using a linear spring with a stiffness of 4 MN/m/m. To investigate the influence of lower toe support, a series of numerical simulations were carried using a FLAC code previously validated against two full-scale walls constructed at RMC: Wall 1 (Figure 4a) constructed with an extensible geogrid and Wall 6 which was nominally identical to Wall 1 but constructed with a relatively inextensible steel welded wire mesh (Huang et al. 2009). Simulations were carried out for a 6 m-high modular block wall with variable toe support stiffness. The results are reproduced in Figure 6. The numerical results show that reinforcement loads are attenuated at the base of the wall as observed in physical wall case studies for toe stiffness values greater than or equal 4 MN/m/m. If the toe stiffness is progressively relaxed in a series of simulations then the distribution of reinforcement loads begins to approach a linear increasing trend with depth below the wall. Nevertheless, while the trend becomes more triangular-shaped the magnitude of reinforcement loads is still less than values pre-

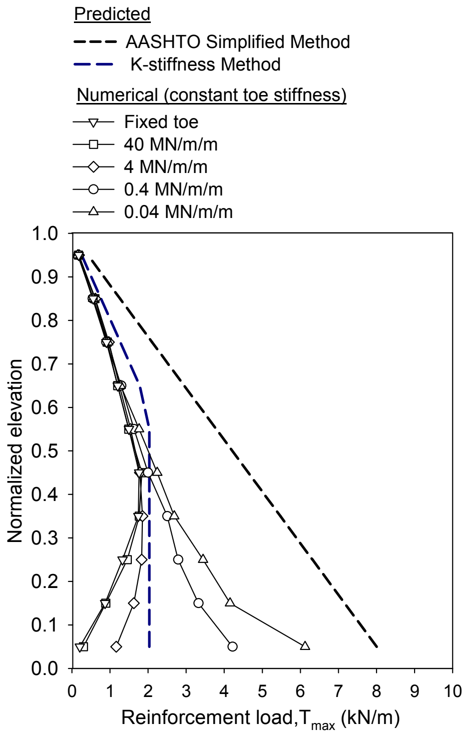

Figure 6. Influence of (constant) toe stiffness on maximum reinforcement loads and comparison with predictions using AASHTO Simplified Method and K-stiffness Method for wall with polyester (PET) reinforcement. (H = 6 m, S_v = 0.6 m, ω = 8 degrees). (after Huang et al. 2010)

dicted using the AASHTO Simplified Method. Hence, the conservatism in predicted reinforcement loads using current practice cannot be explained entirely by toe restraint. Figure 7 shows that for the wall with the least toe support there was not a contiguous internal failure mechanism developed within the reinforced soil mass at the end of construction. This is a necessary condition if the underlying deterministic model in the AASHTO Simplified Method is applicable.

It is possible that interface shear stiffness values greater than 4 MN/m/m would result for a block with a rougher base or a shear key that projects below the base of the block into a granular base material. Taken together, the data shows that significant horizontal toe load capacity is possible through shear transfer at the base of modular block (segmental) walls and a granular leveling pad or concrete footing that is seated in turn on a competent foundation.

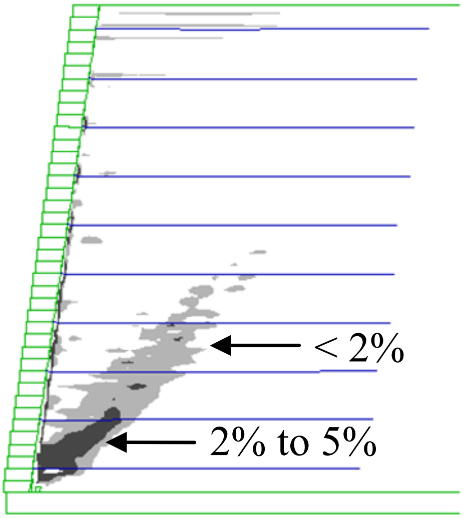

Figure 7. End-of-construction soil shear strain contours for walls with polyester (PET) reinforcement and very low horizontal toe stiffness = 0.04 MN/m/m. (H = 6 m, S_v = 0.6 m, ω = 8 degrees from vertical).

4 K-STIFFNESS METHOD

4.1 *General*

The poor prediction accuracy of current limit equilibrium-based design methods (e.g. AASHTO Simplified Method) prompted the writers and co-workers to develop an empirical-based working stress method to predict reinforcement loads in reinforced soil wall systems. A characteristic feature of this method is the explicit inclusion of the stiffness of the reinforcement; hence, the title "K-stiffness method". The general approach has been adopted for both steel and geosynthetic reinforced soil walls in an attempt to provide a seamless transition between what have historically been treated as two distinct structure categories. However, this paper is restricted to relatively extensible polymeric reinforcement material (geosynthetics).

The K-stiffness Method is an empirical-based method that has been refined from its first variation described by Allen et al. (2003) to its current form as reported by Bathurst et al. (2008b). The evolution of the method has occurred as more quantitative wall performance data has been gathered and the method extended to accommodate cohesive-frictional backfill soils. At the core of the current method is an expression for the maximum reinforcement load (T_{max}) which is expressed as:

$$T_{max} = 0.5K\gamma\,(H+S)S_v\,D_{tmax}\,\Phi_g\,\Phi_{local}\,\Phi_{fs}\,\Phi_{fb}\,\Phi_c \quad (3)$$

Here, H = height of wall and D_{tmax} = load distribution factor that modifies the reinforcement load based on layer location (see bi-linear envelope in Figure 3). The remaining terms Φ_g, Φ_{local}, Φ_{fs}, Φ_{fb} and Φ_c are influence factors that account for the effects of global and local reinforcement stiffness, facing stiffness, face batter and soil cohesion, respectively. The coefficient of lateral earth pressure is calculated as K = 1 - sinϕ with $\phi = \phi_{ps}$ = secant peak plane strain friction angle of the soil. However, it should be noted that parameter K is used as an index value and does not imply that at-rest soil conditions exist in the reinforced soil backfill according to classical earth pressure theory.

The proposed model captures all qualitative effects due to reinforcement stiffness, soil strength, facing stiffness and reinforcement arrangement expected by reinforced soil wall design engineers. Furthermore, the general structure of the model equation may be familiar to geotechnical engineers using classical earth pressure theory in combination with a tributary area approach for the distribution of earth pressures to the internal reinforcement layers. For example, the load carried by a reinforcement layer will decrease as soil friction angle increases (i.e. because the magnitude of coefficient of earth pressure K decreases). The reinforcement load will increase as soil unit weight (γ) and reinforcement spacing (S_v) increases.
Further details of the development of the original K-stiffness Method can be found in the papers by Allen et al. (2003) and Bathurst et al. (2005). The implementation of the original K-stiffness Method for cohesionless backfill soils can be found in the WSDOT (2005) guidance document. Details of each influence factor and its calculation are described next.

Parameter Φ_g is a global stiffness factor that accounts for the influence of the stiffness and spacing of the reinforcement layers over the entire wall height and is calculated as follows:

$$\Phi_g = \alpha(S_{global}/p_a)^{\beta} \quad (4)$$

Here, S_{global} is the global reinforcement stiffness and α and β are constant coefficients equal to 0.25. The non-dimensionality of the expression for global stiffness factor (Φ_g) is preserved by dividing the global reinforcement stiffness by p_a = 101 kPa (atmospheric pressure). The global reinforcement stiffness (S_{global}) accounts for the relative stiffness of the walls and is computed as follows:

$$S_{global} = \frac{\sum J_i}{H} \tag{5}$$

Here, $J_i = J_{2\%}$ is the tensile stiffness, at the end of wall construction, of an individual reinforcement layer expressed in units of force per unit length of wall (see Figure 1). Reinforcement strains in monitored field walls that have behaved well under operational conditions have stayed the same or strain rates have decreased with time after about 1000 hours following end of construction. At longer times there is evidence in some monitored walls of reinforcement load relaxation with time following construction (Allen and Bathurst 2002; Bathurst et al. 2005; Tatsuoka et al. 2004; Kongkitkul et al. 2010). Hence, tensile reinforcement loads at the end-of-construction condition are the maximum loads used in the K-stiffness method provided original site and boundary conditions for which the wall was designed do not change.

The method has been calibrated against measured reinforcement loads deduced from isochronous stiffness values corresponding to 2% strain and elapsed construction times or 1000 hours. The default time of 1000 hours is reasonable in the absence of actual project timelines since most walls are constructed within 1000 hours. Furthermore, results of in-isolation constant load (creep) and constant-rate-of-strain (CRS) tests on the polyolefin reinforcement products used in the case studies have shown that the $J_{2\%}$ secant stiffness is a constant value for practical purposes at or beyond 1000 hours (e.g. Figure 1).

The practical result of the formulation for global stiffness factor (Equation 4) is that as reinforcement stiffness increases and all other factors remain the same, reinforcement load (T_{max} in Equation 3) goes up.

Parameter Φ_{local} is a local stiffness factor that accounts for the relative stiffness of the reinforcement layer with respect to the average stiffness of all reinforcement layers and is expressed as:

$$\Phi_{local} = \left(\frac{S_{local}}{S_{global}}\right)^a \tag{6}$$

where "a" is a constant coefficient and S_{local} is the local reinforcement stiffness for reinforcement layer i calculated as:

$$S_{local} = \left(\frac{J}{S_v}\right)_i \tag{7}$$

Back-fitting of measured versus predicted reinforcement loads by Allen et al. (2003) gave a = 1 for geosynthetic reinforced soil walls. Local deviations from overall trends in reinforcement load can be expected when the reinforcement stiffness and/or spacing of the reinforcement change from average values over the height of the wall (i.e. $S_{local}/S_{global} \neq 1$; Hatami et al. 2001). This effect is captured by the local stiffness factor Φ_{local}.

Parameter Φ_{fb} in the K-stiffness equation accounts for the influence of the facing batter and is computed as:

$$\Phi_{fb} = \left(\frac{K_{abh}}{K_{avh}}\right)^d \tag{8}$$

where, K_{abh} is the horizontal component of active earth pressure coefficient accounting for wall face batter, K_{avh} is the horizontal component of active earth pressure coefficient (assuming the wall is vertical), and "d" is a constant coefficient. The form of the equation shows that as the wall face batter angle $\omega \to 0$ (i.e. wall facing batter approaches the vertical) the facing batter factor $\Phi_{fb} \to 1$. The value of the coefficient term "d" is taken as 0.5.

The influence factor for facing stiffness (rigidity) Φ_{fs} is computed as:

$$\Phi_{fs} = \eta (F_f)^\kappa \tag{9}$$

In the latest version of the K-stiffness Method (Bathurst et al. 2008b) the value of facing column stiffness parameter F_f is calculated as

$$F_f = \frac{1.5H^3 p_a}{Eb^3 (h_{eff}/H)} \tag{10}$$

Here, b = thickness of the facing column, H = height of the facing column (wall), and E = elastic modulus of the "equivalent elastic beam" representing the wall face. The two expressions used to compute the facing stiffness factor show that as the wall becomes higher (H) and less stiff (Eb^3), its rigidity becomes less and hence more load is carried by the reinforcement layers (i.e. Φ_{fs} is larger). A numerical investigation by Rowe and Ho (1997) also predicted that reinforcement loads will increase in a propped panel wall as the stiffness of the facing decreases. This effect has been quantitatively demonstrated using measurements from a pair of full-scale reinforced soil walls tests reported by Bathurst et al. (2006) described earlier. The 3.6 m-high structures were nominally identical except one was built with a relatively stiff modular block facing and the other with a very flexible wrapped-face. The loads in the most heavily loaded reinforcement layers were 3.5 times greater at end of construction than those in the modular block wall.

The term h_{eff} is the equivalent height of an unjointed facing column that is 100% efficient in transmitting moment through the height of the facing column. The ratio h_{eff}/H is used to estimate the efficiency of a jointed facing system to transmit moment along the facing column. Some subjective rules are required to select the value of h_{eff}. For example, during calibration for modular block walls, h_{eff} was taken as 2b where b is the toe to heel dimension of the facing units. For full height and incremental panel walls h_{eff} = H and panel height, respectively. For flexible sand-bag face walls, h_{eff} is taken as S_v (the primary reinforcement spacing). However, if the same sand-bag face is wrapped by the primary reinforcement layers then h_{eff} = H. The non-dimensionality of the facing stiffness factor equation is preserved by the use of p_a = 101 kPa.
Based on back-analyses performed by Bathurst et al. (2008c) the coefficient terms η and κ were determined to be 0.69 and 0.11, respectively.
The effect of soil cohesion is captured by the cohesion (influence) factor ϕ_c computed as:

$$\Phi_c = 1 - \lambda \frac{c}{\gamma H} \qquad (11)$$

where the cohesion coefficient λ = 6.5. Examination of this equation with λ = 6.5 reveals that the practical limit $0 \geq \Phi_c \geq 1$ requires $c/\gamma H \leq 0.153$. It is possible that a combination of a short wall height and high cohesive soil strength could lead to $\Phi_c = 0$. In practical terms this means that no reinforcement is required for internal stability. However, this does not mean that the wall will be stable at the facing (e.g. connection over-stressing may still occur).

The load distribution factor $D_{tmax} = T_{max}/T_{mxmx}$ is used to modify the reinforcement load T_{max} based on layer location. Parameter T_{mxmx} is the maximum reinforcement load from all reinforcement layers. The distribution of D_{tmax} plotted against normalized height of wall is trapezoidal in shape as originally proposed by Allen et al. (2003) or can be assumed to be bi-linear as plotted Figure 3. The value of T_{mxmx} can be calculated by setting D_{tmax} = 1 in the K-stiffness Method equation. The observation that the distribution of reinforcement loads is bi-linear is not new. A bi-linear distribution was proposed by Collin (1986) for geogrid reinforced soil walls.

Further discussion regarding the selection of parameters in the K-stiffness Method equations can be found in the earlier papers by Allen et al. (2003) and Miyata and Bathurst (2007) and the WSDOT (2005) design guidance document.

4.2 *Calibration*

The K-stiffness Method is an empirical-based working stress design method. The influence factors and coefficients which appear in the equations introduced above were determined by back-fitting to measured loads using conventional optimization schemes (see Bathurst et al. 2008b). However, only reinforcement loads from walls that were judged to exhibit good performance were considered for the database used for calibration. Good performance was defined as:

- Reinforcement strains are small (typically less than 3%).
- Creep strains and strain rates decrease with time (i.e. only primary creep occurs).
- The wall backfill soil does not exhibit signs of failure (cracking, slumping, etc.).
- For frictional soils, post-construction deformations, which are typically greatest at the wall top, are less than 30 mm within the first 10,000 h.
- For cohesive-frictional soils, post-construction deformations are not greater than 300 mm or 3% of the height of the wall, whichever is less (PWRC 2000).

4.3 *Internal soil failure limit state*

An important and unique feature of the K-stiffness Method is the introduction of an internal soil *failure* limit state. The calibration of the method has been based on the requirement that a contiguous failure mechanism must not develop through the reinforced soil zone. This has been achieved by limiting the maximum strain in the reinforcement to 3% based on load-time-strain performance of the reinforcing layers in geosynthetic reinforced soil walls. This is an important difference from the Simplified Method and variants that assume that the soil and reinforcement reach failure simultaneously. The latter is a rare if not impossible scenario for extensible geosynthetic reinforcement materials. When wall failure has been generated in RMC full-scale walls constructed with geosynthetic reinforcement, the granular soil has always failed first. Hence, designing to prevent soil failure is rational and safe, and at the same time ensures good performance as defined by the criteria identified earlier. Stated alternatively, by designing to prevent failure of the soil in the reinforced soil zone it is not possible to reach a failure limit state for the reinforcement (rupture or over-stressing).

4.4 *Accuracy of the K-stiffness Method*

The same database of measured reinforcement loads used to investigate the accuracy of the AASHTO Simplified Method was used by Bathurst et al. (2008c) to quantify the accuracy of the K-stiffness Method. The results are reproduced in Figures 8. Data for walls with cohesive-frictional and frictional soil backfills are included in this figure. The load bias statistics are almost the same for both data sets. The plots show that the data are distributed much closer to the 1:1 reference line than the corresponding data using the current AASHTO (2002) Simplified Method (Figure 2). Additional results of numerical simulations are shown in Figure 9. The data show that the K – stiffness Method does well in conservatively capturing the measured load data for a range of wall heights and reasonable estimates of toe stiffness.

4.5 *Applicability of K-stiffness Method*

The K-stiffness Method is empirically based with parameters that have been determined by calibration against a database of carefully constructed, instrumented and monitored structures. An important implication of this approach is that the method can only be used for structures with properties and boundary conditions that fall within the envelope of case study properties that were used to perform the calibration. For example, the wall heights in the database vary from 3 to 12.6 m. Hence, using the K-stiffness Method to design walls of greater height should be carried out with caution. A total of 22 walls were built in the field on natural soils or on a depth of foundation soil in the laboratory. The remaining nine were built on rigid foundations. Hence, the K-stiffness Method is applicable to walls built on typical competent foundations where the performance of the structures is not influenced by excessive settlements or failure of the foundation or wall toe. Similar foundation criteria apply to the tie-back wedge approach (i.e. Simplified Method) for the calculation of internal reinforcement loads (e.g. AASHTO 2002; FHWA 2001; CFEM 2006; NCMA 2009).

A total of 21 wall sections were constructed with a vertical face; the remaining walls were constructed with facing batter (ω) from 3° to 27°. Most of the walls were constructed with a hard structural facing. A total of 58 data points were collected from 13 wall sections built with cohesionless soils and 79 data points from sections built with cohesive-frictional soils.

The K-stiffness Method in its most current form accounts for the positive contribution of soil cohesion to reduce geosynthetic reinforcement loads (Bathurst et al. 2008c). In many parts of the world purely frictional (granular) soils are not available and ignoring the cohesive component of available

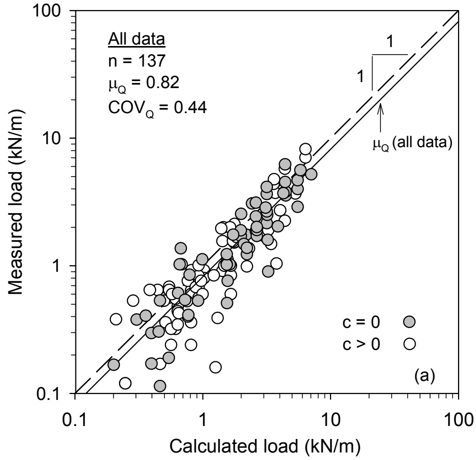

Figure 8. Measured versus calculated reinforcement loads using the K-stiffness Method.

cohesive-frictional soils will lead to uneconomical structures. Nevertheless, the engineer of record must be familiar with project backfill soils and must decide if the cohesive component of soil strength used to compute the cohesion influence factor (Φ_c) is available for the life of the structure. If this strength component cannot be guaranteed, the K-stiffness Method should be used with $\phi > 0$ and $c = 0$. This will result in a conservative (safe) design.

Finally, it must be recalled that the K-stiffness Method was developed to compute reinforcement loads used for the internal stability design of reinforced soil retaining walls. At present the method applies only to internal rupture (over-stressing) and pullout failure modes (or limit states). Other failure modes related to facing column stability, external stability and possible failure mechanisms that pass partially through the reinforced soil mass are beyond the scope of the method. For these failure modes current limit equilibrium-based models together with conventional factors of safety are available. The influence of additional loads due to earthquake has yet to be addressed within the K-stiffness Method framework.

5 LIMIT STATES DESIGN

5.1 *General*

Limit states design (LSD) (called load and resistance factor design (LRFD) in North America) has been used in structural engineering for decades. It is now recommended in American Association of State Highway and Transportation Officials design specifications (AASHTO 2007, 2009) and the

Canadian Highway Bridge Design Code (CHBDC 2006) for the design of foundations and earth retaining structures in transportation-related structures. Included in the category of earth retaining structures are steel and geosynthetic reinforced soil wall systems.

In load and resistance factor design, engineers use prescribed limit state equations and load and resistance factors specified in design codes to ensure that a target probability of failure for each load carrying member in a structure is not exceeded. The preferred objective of LSD calibration is to compute load and resistance factor values to meet a target probability of failure using *measured* load and resistance data rather than fitting to allowable stress design (ASD) past practice. The methodology to carry out LSD calibration recommended by AASHTO is described in a guidance document prepared Allen et al. (2005). Additional recommendations are found in the paper by Bathurst et al. (2008a). The fundamental limit state expression used in LRFD is:

$$\varphi R_n \geq \sum \gamma_i Q_{ni} \tag{12}$$

Here, Q_{ni} = nominal (specified) load; R_n = nominal (characteristic) resistance; γ_i = load factor; and φ = resistance factor. In design codes, load factor values are typically greater than or equal to one and resistance factor values are always less than or equal to one.

It is important to emphasize that for bridge design, a nominal load is not a failure load but rather a value that is a best estimate of the load under *operational conditions* (Harr 1987). For example, this nominal load may be due to structure dead loads plus a representative vehicle load based on statistical treatment of bridge traffic. Conceptually, the margin of safety is largely provided by the resistance side of the equation where the resistance value is calculated based on the failure capacity (ultimate limit state) or a deformation criterion (serviceability limit state) for each element analyzed. For the case of a steel member, the ultimate resistance of the member is based (typically) on flexure or shear capacity, and serviceability on a prescribed allowable deformation.

The same concepts described above must apply to strength limit states for internal stability design of geosynthetic reinforced soil walls using LRFD (e.g. rupture (over-stressing) and pullout). The reinforcement loads due to soil self-weight can be estimated using the current AASHTO (2007, 2009) Simplified Method. A common source of confusion and conflict with LSD using the Simplified Method is that the underlying deterministic model to calculate reinforcement loads is based on active

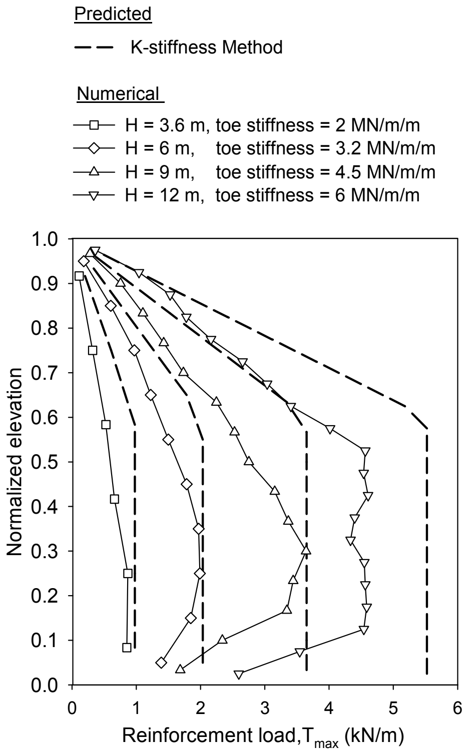

Figure 9 Influence of toe stiffness and wall height on maximum reinforcement loads and comparison with predictions using K-stiffness Method for modular block wall with PET reinforcement. (S_v = 0.6 m, ω = 8 degrees).

earth pressure theory or Coulomb wedge analysis and hence the soil and critical reinforcement layers are assumed to be simultaneously at incipient failure. Even if this unlikely coincidence was accepted *a priori* at an ultimate limit state, measured loads are typically very much lower than loads predicted using methods extrapolated from classical active earth pressure theory (i.e. Simplified Method and variants) as discussed earlier in this paper. Furthermore, there is a body of physical evidence that tensile reinforcement loads at the end-of-construction condition are the maximum loads for internal LSD provided original site and boundary conditions for which the wall was designed do not change.

5.2 *Selection of target probability of failure P_f*

The objective of limit states design calibration using reliability theory is to select values of resistance factor and load factor(s) such that a target probability of failure is achieved for the limit state function. The target probability of failure is taken as 1 in 100 (P_f = 0.01) which corresponds to a reliability index value β = 2.33. This target P_f value has been recommended for reinforced soil wall structures because they are redundant load capacity systems (Allen et al. 2005). If one layer fails in pullout, load is shed to the neighboring reinforcement layers. Pile groups are another example of a redundant load capacity system; failure of one pile does not lead to failure of the group because of load shedding to the remaining piles. In the USA, pile groups are also designed to a target reliability index value of $\beta = 2.33$.

5.3 *Influence of load model on LRFD calibration*

Despite the shortcomings of limit equilibrium-based methods for the design of geosynthetic reinforced soil walls noted above in the context of observed behavior and LSD calibration, the Simplified Method is the only method currently available in AASHTO (2007, 2009) and FHWA (2001) guidance documents to estimate tensile loads in geosynthetic reinforcement layers. However, the poor prediction accuracy of the model renders proper LSD calibration problematic if calibration is carried out using measured reinforcement load data. The limit state equation for pullout assuming loads are due to soil self-weight plus uniformly distributed surcharge can be expressed as:

$$\varphi P_c - \gamma_Q T_{max} \geq 0 \tag{13}$$

Here, P_c is pullout capacity and φ and γ_Q are resistance and load factors, respectively. In current AASHTO (2007, 2009) codes $\gamma_Q = 1.35$ for loads due to soil self-weight plus uniformly distributed surcharge. LSD calibration using the Simplified Method results in a resistance factor $\varphi > 1$ which is not acceptable.

The corresponding limit state equation for reinforcement rupture (over-stressing) can be written as:

$$\varphi T_{al} - \gamma_Q T_{max} \geq 0 \tag{14}$$

where the (nominal) available long-term tensile strength (T_{al}) of each geosynthetic reinforcement layer is computed as follows:

$$T_{al} = \frac{T_{ult}}{RF} = \frac{T_{ult}}{RF_{ID} \times RF_{CR} \times RF_D} \tag{15}$$

In this expression, T_{ult} = ultimate tensile strength of the reinforcement and RF = product of reduction factors to account for potential long-term strength loss due to installation damage (RF_{ID}), creep (RF_{CR}) and degradation due to chemical/biological processes (RF_D).

A non-sensible resistance factor ($\varphi > 1$) also results when reliability-based LSD calibration is carried out using measured loads and measured bias statistics for strength reduction processes. However, when the K-stiffness Method is used to compute reinforcement loads at end of construction (i.e. operations conditions), the computed resistance factor for pullout and rupture limit states are typically $\varphi = 0.70$ and 0.55, respectively. There are small variations in these values depending on the type of geosynthetic, but in all cases the values are judged to be reasonable since they are less than one.

6 CONCLUSIONS

There is now a large and irrefutable body of physical data that shows that current limit equilibrium-based design models for the calculation of reinforcement loads under operational conditions are excessively conservative and inaccurate with respect to the distribution of reinforcement loads. Current tie-back wedge methods and variants should be recognized as simple models that are neither rational nor theoretically consistent within a mechanics framework. Their use is complicated by difficulties relating loads at soil failure (plasticity) to working stress conditions and the assumption that the soil and reinforcement fail simultaneously. Furthermore, geosynthetic reinforced soil walls are systems with complex interactions between the soil, visco-elastic-plastic polymeric reinforcement elements, discrete structural facing columns and toe boundary conditions. The notion that accurate closed-form analytical solutions are possible based on the mechanics of these complex systems is, in the opinion of the writers, not realistic. Nevertheless it is recognized that safe designs do result using current limit equilibrium-based load models if ASD past practice is adopted. Unfortunately, ASD past practice does not provide the designer with an estimate of the actual margin of safety (or probability of failure) for each mode of failure. This is not the case for the design of related engineering structures (e.g. bridge superstructures which are often supported by retaining wall abutments). However, the excessive conservatism and poor prediction accuracy of limit equilibrium-based load models renders reliability-based limit states design calibration for resistance factors impossible. Hence the use of these load models is an impediment to the migration of internal stability design for geosynthetic reinforced soil walls to a modern limit states design framework and future performance-based design. The development of properly formulated limit states design equations with acceptable probabilities of failure are required if reinforced soil retaining walls structures are to be designed within the same limit states design framework currently used for piled foundations and buildings. The K-stiffness Method quantitatively captures the influence of soil properties, reinforcement properties and structural wall facings on the magnitude of reinforcement loads under operational conditions and this leads to reasonable values for load and resistance factors. At the time of writing the K-stiffness Method offers the only framework for reliability-based limit states design calibration for rupture and pullout internal limits for geosynthetic reinforced soil walls.

REFERENCES

AASHTO. 2002. Standard Specifications for Highway Bridges. American Association of State Highway and Transportation Officials (AASHTO), 17th ed., Washington, D.C.

American Association of State Highway and Transportation Officials (AASHTO). 2007. LRFD Bridge Design Specifications. 4th edition, Washington, DC, USA.

American Association of State Highway and Transportation Officials (AASHTO). 2009. Interim LRFD Bridge Design Specifications. 4th edition, Washington, DC, USA.

Allen, T.M. and Bathurst, R.J. 2002. Soil reinforcement loads in geosynthetic walls at working stress conditions, Geosynthetics International, Vol. 9(5-6), pp. 525-566.

Allen, T.M., Bathurst, R.J. and Berg, R.R. 2002. Global level of safety and performance of geosynthetic walls: An historical perspective, Geosynthetics International, Vol. 9(5-6), pp. 395-450.

Allen, T.M., Bathurst, R.J., Holtz, R.D., Lee, W.F. and Walters, D.L. 2004. A new working stress method for prediction of loads in steel reinforced soil walls, ASCE Journal of Geotechnical and Geoenvironmental Engineering. Vol. 130(11), pp. 1109-1120.

Allen, T.M., Bathurst, R.J., Walters, D.L., Holtz, R.D. and Lee, W.F. 2003. A new working stress method for prediction of reinforcement loads in geosynthetic walls, Canadian Geotechnical Journal, Vol. 40(5), pp. 976-994.

Allen, T.M. and Holtz, R.D. 1991. Design of retaining walls reinforced with geosynthetics, Geotechnical Engineering Congress 1991, McLean, F., Campbell, D.A., and Harris, D.W., Editors, ASCE Geotechnical Special Publication No. 27, Vol. 2, Proceedings of a congress held in Boulder, Colorado, USA, June 1991, pp. 970-987.

Bathurst, R.J., Allen, T.M. and Nowak, A.S. 2008a. Calibration concepts for load and resistance factor design (LRFD) of reinforced soil walls, Canadian Geotechnical Journal Vol. 45(10), pp. 1377–1392.

Bathurst, R.J, Allen, T.M. and Walters, D.L. 2005. Reinforcement loads in geosynthetic walls and the case for a new working stress design method, Geotextiles and Geomembranes, Vol. 23(4), pp. 287-322.

Bathurst, R.J., Nernheim, A. and Allen, T.M. 2009. Predicted loads in steel reinforced soil walls using the AASHTO Simplified Method, ASCE Journal of Geotechnical and Geoenvironmental Engineering, Vol. 135(2), pp. 177-184.

Bathurst, R.J., Nernheim, A. and Allen, T.M. 2008b. Comparison of measured and predicted loads using the Coherent Gravity Method for steel soil walls, Ground Improvement, Vol. 161(3), pp. 113-120.

Bathurst, R.J., Miyata, Y., Nernheim, A. and Allen, T.M. 2008c. Refinement of K-stiffness Method for geosynthetic reinforced soil walls, Geosynthetics International, Vol. 15(4), pp. 269-295.

Bathurst, R.J., Vlachopoulos, N., Walters, D.L., Burgess, P.G. and Allen, T.M. 2006. The influence of facing rigidity on the performance of two geosynthetic reinforced soil retaining walls, Canadian Geotechnical Journal, Vol. 43(12), pp. 1225-1237.

BS8006. 1995. Code of practice for strengthened/reinforced soil and other fills, British Standards Institution, Milton Keynes, United Kingdom.

Canadian Foundation Engineering Manual (CFEM). 2006. Canadian Geotechnical Society, 4th edition, BiTech Publishers, Richmond, BC, Canada.

Canadian Highway Bridge Design Code (CHBDC). 2006. CSA Standard S6-06, Canadian Standards Association (CSA), Toronto, Ontario, Canada.

Christopher, B.R. 1993. Deformation response and wall stiffness in relation to reinforced soil wall design, Ph.D. Dissertation, Purdue University, West Lafayette, Indiana, USA.

Christopher, B.R., Gill, S.A., Giroud, J.-P., Juran, I., Mitchell, J.K., Schlosser, F. and Dunnicliff, J. 1990. Reinforced Soil Structures: Volume I. Design and Construction Guidelines, Report No. FHWA-RD-89-043, Washington, DC, USA.

Collin, J.G. 1986. Earth wall design. Ph.D. thesis, University of California, Berkeley, California, USA.

Federal Highway Administration (FHWA). 2001. Mechanically Stabilized Earth Walls and Reinforced Soil Slopes — Design and Construction Guidelines. FHWA-NHI-00-043, (editors Elias, V., Christopher, B.R., Berg, R.R.). Federal Highway Administration, Washington, DC, USA.

Geoguide 6. 2002. Guide to reinforced fill structure and slope design, Geotechnical Engineering Office, Hong Kong, China.

Harr, M.E. 1987. Reliability-Based Design in Civil Engineering. McGraw-Hill Book Company, New York, NY, USA.

Hatami, K., Bathurst, R.J. and Di Pietro, P. 2001. Static response of reinforced soil retaining walls with non-uniform reinforcement, International Journal of Geomechanics, Vol. 1(4), pp. 477-506.

Huang, B., Bathurst, R.J. and Hatami, K. 2009. Numerical study of reinforced soil segmental walls using three different constitutive soil models, ASCE Journal of Geotechnical and Geoenvironmental Engineering, Vol. 135(10), pp. 1486-1498.

Huang, B., Bathurst, R.J., Hatami, K. and Allen, T.M. 2010. Influence of toe restraint on reinforced soil segmental walls, Canadian Geotechnical Journal (in press).

Koerner, J., Soong, T.-Y. and Koerner, R.M. 1998. Earth retaining wall costs in the USA. Geosynthetic Institute, Folsom, PA, USA.

Kongkitkul, W., Tatsuoka, F., Hirakawa, D., Sugimoto, T., Kawahata, S. and Ito, M. 2010. Time histories of tensile force in geogrid arranged in two full-scale high walls, Geosynthetics International, Vol. 17(1), (in press).

Leshchinsky, D. and Han, J. 2003. Reinforced Multitiered Walls, Report DCT 158. Delaware Center for Transportation, University of Delaware, Newark, Delaware, USA.

Miyata, Y. and Bathurst, R.J. 2007. Development of K-stiffness Method for geosynthetic reinforced soil walls constructed with c-ϕ soils, Canadian Geotechnical Journal, Vol. 44(12), pp. 1391-1416.

NCMA. 2009. Design Manual for Segmental Retaining Walls (3rd edition). National Concrete Masonry Association, (ed. M. Bernardi), Herndon, VA, USA.

Public Works Research Center (PWRC). 2000. Design and Construction Manual of Geosynthetics Reinforced Soil (revised version), Public Works Research Center, Tsukuba, Ibaraki, Japan, 305 p. (in Japanese).

Rowe, R.K. and Ho, S.K. 1993. Keynote Lecture: A review of the behavior of reinforced soil walls, Earth Reinforcement Practice, Ochiai, H., Hayashi, S. and Otani, J., Editors, Balkema, 1993, Proceedings of the International Symposium on Earth Reinforcement Practice, Vol. 2, Kyushu University, Fukuoka, Japan, November 1992, pp. 801-830.

Rowe, R.K. and Ho, S.K. 1997. Continuous panel reinforced soil walls on rigid foundations, Journal of Geotechnical and Geoenvironmental Engineering, Vol. 123(10), pp. 912–920.

Tatsuoka, F., Hirakawa, D., Shinoda, M., Kongkitkul, W. and Uchimura, T. 2004. An old but new issue; viscous properties of polymer geosynthetic reinforcement and geosynthetic-reinforced soil structures. Keynote Lecture. In Proceedings of the 3rd Asian Regional Conference on Geosynthetics (GeoAsia 2004, editors: Shim, J. B., Yoo, C. and Jeon, H.-Y.), Seoul, Korea, pp. 29–77.

Walters, D.L., Allen, T.M. and Bathurst, R.J. 2002. Conversion of geosynthetic strain to load using reinforcement stiffness, Geosynthetics International, Vol. 9(5-6), pp. 483-523.

WSDOT. 2005. Geotechnical Design Manual M46-03, Washington State Department of Transportation, Tumwater, WA, USA.

Whitcomb, W. and Bell, J.R. 1979. Analysis techniques for low reinforced soil retaining walls and comparison of strip and sheet reinforcements, Proceedings of the 17th Engineering Geology and Soils Engineering Symposium, Moscow, Idaho, USA, pp. 35-62.